

Efficient Spatial Dataset Search over Multiple Data Sources

Wenzhe Yang, Sheng Wang, Yuan Sun, Zhiyu Chen, Zhiyong Peng

Abstract—In this paper, we investigate a novel spatial dataset search paradigm over multiple spatial data sources, which enables users to conduct join and union searches seamlessly. Specifically, we define two search problems called Maximum Intersection Query (MIQ) and Maximum Coverage Query with a Connection constraint (MCQC). To address these problems, we propose a unified Multi-source Spatial Dataset Search (MSDS) framework. In MSDS, we design a multi-layer index to accelerate the MIQ and MCQC. In addition, we prove that the MCQC is NP-hard and design two greedy algorithms to solve the problem. To deal with the constant update of spatial datasets in each data source, we design a dynamic index updating strategy and optimize search algorithms to reduce communication costs and improve search efficiency. We evaluate the efficiency of MSDS on five real-world data sources, and the experimental results show that our framework is able to achieve a significant reduction in running time and communication cost.

Index Terms—Spatial dataset search, set intersection, maximum coverage problem, NP-hard.



1 INTRODUCTION

In the last decade, datasets have become an essential factor of production. To improve the availability of datasets, researchers have a great interest in dataset search [10, 20, 26, 46] and many dataset search systems have been developed, such as Aurum [22], Auctus [13], Ronin [33], and many others [12, 36]. The most popular way to find datasets is based mainly on keywords or catalogs in the available metadata [14, 26]. However, the insufficient metadata information makes it difficult for users to find a dataset. Therefore, motivated by exemplar search [31], we study a search paradigm to find datasets of interest by entering an exemplar dataset [46].

Spatial data, as one of the most important components of real-world data, is one of the most critical factors supporting decision-making in many fields. So search based on spatial datasets has been used in a wide variety of industries and provides invaluable insight, such as transportation planning [43], business decisions, diseases prevention [4], motion prediction [28], and so on. This suggests that conducting research on spatial dataset search is essential for discovering and reusing spatial data to help with prediction, analysis, and decision-making.

However, massive spatial data often come from different data sources and are located in different regions. Many open-source data platforms, such as OpenGeoMetadata [3], GeoBlacklight [1], OpenGeoHub [2], etc., integrate spatial data from multiple open data sources. Also, individual companies or organizations are independent in managing datasets and have a wealth of spatial data stored in their own data sources. It is crucial to break the barriers of different data sources to facilitate the spatial dataset search from different data sources. Motivated by this, we focus on

the spatial dataset search problem over multiple data sources to support the effectiveness and efficiency of the search in this paper.

As a fundamental and essential operation in spatial dataset search, spatial join search has been widely studied [13, 35, 47, 51, 53], among which set intersection is one of the most commonly used metrics to measure joinability [13, 35, 51]. In addition, union search is also important in dataset search as a way to extend and enhance the query data [32]. However, how to find unionable spatial datasets has not been fully explored. Considering the spatial dataset search scenario, spatial proximity (or connectivity) [7, 25, 43] and the size of unionable (or extensible) [7, 25] data points are two key factors indicating the unionability of two spatial datasets. Thus, we propose a new class of spatial union search based on the set coverage problem and connectivity constraint.

Currently, the spatial dataset join and union searches have been widely used in many applications. For example, in transportation planning [43], passengers can find unionable spatial datasets that maximize the weighted sum of transit network connectivity and commuting demand. In remote sensing, people often search for joinable datasets from multiple sensors for data fusion [50]. In disease prevention, epidemiologists can find k joinable spatial datasets of diseases with similar distributions to analyze correlations between diseases [4]. In biological sciences, researchers can track animals by finding overlapping motion tracks to reveal patterns of behavior [39]. Below is a concrete example of a multi-source spatial dataset search in transportation planning.

Example 1. *The public transport in each city is made up of multiple transport companies with different modes, such as bus companies, subway companies, etc. The high levels of traffic congestion have seriously impacted people’s lives. In this context, one of the government’s solutions is to integrate different modes of transport and construct sound public transport. For example, in a public transit system made up of datasets from multiple sources, including buses, subways, and waterways in Washington D.C. and Maryland. Fig. 1(a) shows a subway line Q in Washington D.C. (1) To improve the efficiency of public transport, we need to find those with highly overlapping lines but different modes of*

- Wenzhe Yang and Sheng Wang are with the School of Computer Science, Wuhan University, China. Email: {wenzheyang, swangcs}@whu.edu.cn.
- Zhiyong Peng is with the School of Computer Science and Big Data Institute, Wuhan University, China. Email: peng@whu.edu.cn.
- Yuan Sun is with La Trobe Business School, La Trobe University, Australia. Email: yuan.sun@latrobe.edu.au.
- Zhiyu Chen is with Amazon in Seattle, USA. E-mail: zhiyu@amazon.com.

Manuscript received xxxx xx, 2023; revised xxxx xx, 2023.

transport and integrate them to improve the efficiency of public transport networks [19]. Fig. 1(b) shows the top-4 routes with the highest overlapping with Q through a join search. From Fig. 1(b) we can find that the subway line Q and bus line D_1 are highly overlapping, so it is possible to consider merging the two lines to reduce the transport costs. (2) To improve the completeness of public transport, we need to expand the coverage region of access to public transport to serve more people [7, 25]. It should be noted that it is inappropriate for the user to commute too long when switching transportation. Thus, a natural concern is to ensure the connection between different routes. As shown in Fig. 1(c), for the given subway line Q in Washington D.C., we can find top-4 bus lines in Maryland with the maximum coverage through union search, and they are connected with Q , so they can meet the intercity commuting needs.

To provide spatial dataset join and union search simultaneously, the implementation of spatial dataset search over multiple data sources faces several key challenges. The first challenge is the high search complexity. Each data source contains large-scale datasets, and we prove that the problem of finding the maximum coverage with connectivity constraints in spatial union search is NP-hard. Hence, how to design efficient indexes and algorithms to accelerate the search process is critical. The second challenge is high communication costs due to limited bandwidth. Moreover, new spatial datasets are constantly emerging in each local data source, and the existing datasets are continually updating [22].

To overcome the above two challenges, we propose an effective **M**ulti-source **S**patial **D**ataset **S**earch (MSDS) framework to support spatial join and union searches, dynamic update of indexes, and maintain up-to-date top- k results for the query. Overall, the contributions of the paper are summarized as follows:

- We define a novel spatial dataset join and union search paradigm over multiple data sources, which seamlessly supports two queries called MIQ and MCQC. We prove the NP-hardness of the MCQC (see Section 3) and develop a unified MSDS framework to support both queries (see Section 4).
- Based on rasterization, we design a multi-layer index composed of a local index called IBtree, a global index, and a dataset graph, which not only accelerates the MIQ and MCQC but also supports dynamic index update (see Section 5).
- We design the query distribution strategies to reduce the communication cost, a search algorithm based on the IBtree, and two greedy heuristic algorithms to accelerate the MIQ and MCQC, respectively (see Section 6). To support dataset update, we design an index’s update strategy and optimize our search algorithms (see Section 7).
- We conduct extensive experimental evaluations over five spatial data sources to verify the index construction, search performance, communication cost of MSDS in solving the MIQ and MCQC (see Section 8).

2 RELATED WORK

Dataset Search. To realize the full potential of the datasets, dataset search arises as one foundational work. According to different data sources, we roughly divide the dataset search into centralized search [32, 37, 42, 46] and distributed search [35, 45, 48]. The existing centralized dataset search studies mainly focus on a local data source or downloading datasets from multiple data sources to a local server, then designing an efficient search

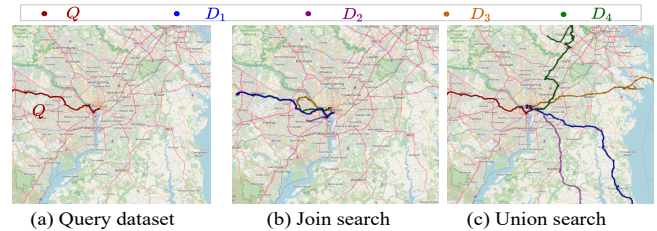


Fig. 1. An example of performing join and union searches on real multi-source transit datasets in Washington, D.C. and Maryland.

framework. For example, Nargesian et al. [32] proposed a solution for finding union tables and downloaded datasets from three data repositories for searching. Wang et al. [42] proposed a search engine search top- k similar trajectory in a taxi trajectory repository. Yang et al. [46] proposed a dual-filtering framework in a local server to support the efficient spatial dataset similarity search.

However, in the real world, most data comes from different organizations or institutions. Due to the geographically dispersed characteristics of the different data sources, several distributed query framework [35, 45, 48] is proposed. A distributed system consists of a cluster of computers in which one computer is the master node, and the others are slave nodes. In traditional distributed search [5, 21, 48], multi-source data first needs to be stored on HDFS. Then the master node partitions all data into chunks of equal size and distributes the data partition to slave nodes. However, in our application scenario, each data source’s datasets are collected by the organization or company and stored on its own servers; each data source is autonomous. Thus, the traditional distributed search solutions are not suitable for our multi-source spatial dataset search scenarios.

Set Intersection. The problem of similarity search on datasets can be formulated as a set similarity search problem, where the similarity measure is the intersection size of sets. Compared with complex similarity measures such as earth mover’s distance [46] and Hausdorff distance [4], the set intersection is simple to compute and understand. Thus, we can consider two sets are similar if their intersection number exceeds a user-defined distance threshold. Currently, the computation of set intersection has received much attention from academia [11, 34, 52] and industry [8, 9], and many techniques have been developed.

Peng et al. [34] transformed time series datasets into sets and measured the similarity based on the Jaccard metric. However, it requires scanning all datasets and estimating the number of set intersections, where pairwise comparisons are time-consuming. Zhu et al. [52] proposed an algorithm called Josie to accelerate the set intersection computation for large-scale sets. However, it assumes that the intersecting tokens between two sets are uniformly distributed, which can result in a less accurate estimated value. Ding et al. [18] proposed partitioning the set into fixed or randomized widths. Then it computes the intersection using the mapping value of each original set under a universal hash function.

Maximum Coverage Problem. The maximum coverage problem (MCP) is a classical problem in combinatorics [27]. Given a universe of elements $\mathcal{U} = \{e_1, e_2, \dots, e_n\}$ and a collection of sets $\mathcal{S} = \{S_1, S_2, \dots, S_m\}$, where each S_i is a subset of \mathcal{U} , the objective of the MCP is to select a fixed number (k) of sets, such that the total number of elements covered by the selected sets is maximized. The MCP has been proven to be NP-hard [27].

Over the past two decades, the MCP has been extensively studied, with many MCP variants proposed. Vazirani et al. [38]

proposed a weighted MCP, where each element in \mathcal{U} has a weight, and the objective is to maximize the total weights of the covered elements. Khuller et al. [29] added budget constraints to MCP, assigning each set a cost. The goal is to select a combination of sets to maximize the number of covered elements without violating budget constraints. The generalized MCP [17] can be regarded as a combination of the above two variants. However, in the generalized MCP, the weight of an element is not predetermined but depends on which collection covers it.

Remarks. The challenges of spatial dataset search over multiple data sources are three-fold: 1) there is no efficient framework to support spatial dataset join and union searches; 2) solving spatial dataset search based on set coverage is highly complex because it is NP-hard; and 3) the search process has high communication cost due to frequent interactions.

3 DEFINITIONS

3.1 Data Models

Definition 1. (Spatial Dataset) A spatial dataset D contains a sequence of points marked with spatial locations, i.e., $D = \{(lat_1, lon_1), (lat_2, lon_2), \dots, (lat_{|D|}, lon_{|D|})\}$.

Definition 2. (Spatial Data Source) A spatial data source \mathcal{D} contains a set of spatial datasets, i.e., $\mathcal{D} = \{D_1, D_2, \dots, D_{|\mathcal{D}|}\}$, $|\mathcal{D}|$ denotes the dataset scale of this source.

Considering each spatial dataset contains plenty of points, it is time-consuming to perform pairwise point matching if measuring the intersection or coverage between datasets. Thus, we utilize a *rasterization* method [49] to construct a compression representation of the spatial dataset. We initialize a 2D space with a minimum coordinate point, and the size of space is $h \times w$, as shown in Fig. 2(a). Then we divide the whole space into a $2^{\theta_1} \times 2^{\theta_2}$ grid, and θ called resolution. We rasterize the space using a cell of size $\mu \times \nu$, where $\mu = h/2^{\theta_1}$ and $\nu = w/2^{\theta_2}$. Each point of the spatial dataset can be mapped to the cell of the grid, whose coordinates are $(\lfloor (lon_i - x_0)/\nu \rfloor, \lfloor (lat_i - y_0)/\mu \rfloor)$. We use the Z-order curve [34, 46] to transform the coordinates of each cell into an integer (Zid) that uniquely identifies the cell. Therefore, each spatial dataset can be represented as a finite set consisting of a sequence of cell IDs. The spatial set is defined as:

Definition 3. (Spatial Set) A spatial set $S_D = \{d_1, d_2, \dots, d_{|S_D|}\}$ denotes the compression representation of dataset D , and d_i is an identifier representing a cell in the plane, and spatial points in D falling inside the same cell are represented by one identifier.

Definition 4. (Spatial Set Distance) Given a query set $S_Q = \{q_1, q_2, \dots, q_{|S_Q|}\}$ and a spatial set $S_D = \{d_1, d_2, \dots, d_{|S_D|}\}$, the distance between the two sets is defined as:

$$dist(S_Q, S_D) = \min\{\|q_i, d_j\|_2 : q_i \in S_Q, d_j \in S_D\}. \quad (1)$$

where q_i and d_j denote cell IDs, which can be decomposed into coordinates in the grid, $\|\cdot\|_2$ is the Euclidean distance.

Definition 5. (δ -Connectivity) Two spatial sets S_Q and S_D are connected if $dist(S_Q, S_D) \leq \delta$, where δ is a user-defined connectivity threshold.

Definition 6. (Connected Graph) Given a collection of spatial sets $\mathcal{S} = \{S_1, S_2, \dots, S_{|\mathcal{S}|}\}$, the undirected graph $G(V, E)$ is constructed from \mathcal{S} , where each node N_i represents a spatial set

TABLE 1: Summary of notations.

Symbol	Description
\mathcal{D}	a data source consisting a set of spatial datasets
$S^{\mathcal{D}}$	a collection of spatial sets in \mathcal{D}
$ \mathcal{D} $	the number of datasets in \mathcal{D}
Q, S_Q	query dataset, query set after rasterization
D, S_D	spatial dataset in \mathcal{D} , spatial set after rasterization
\mathcal{S}	the collection of spatial sets
\mathcal{R}	the collection of result sets
N_Q	the query dataset node
N_R, N_I, N_D	root node, internal node, dataset node
f	the capacity of leaf node
$dist(S_{D_1}, S_{D_2})$	the distance between S_{D_1} and S_{D_2}
h, w	the height and width of the whole 2D space
μ, ν	the height and width of each entry in the grid
2^θ	the number of entries in each dimension

S_i , and each undirected edge $e(i, j)$ represents that two nodes composed of two spatial sets are connected. The graph G is a connected graph if and only if $\forall N_i, N_j \in V (i \neq j)$, there exists a path $P = \langle N_i, \dots, N_j \rangle$ from N_i to N_j .

Example 2. As shown in Fig. 2(b), for three given spatial sets $S_1 = \{d_{11}, d_{12}\}$, $S_2 = \{d_{21}, d_{22}\}$ and $S_3 = \{d_{31}, d_{32}\}$. According to Definition 4, $dist(S_1, S_2) = \|d_{11}, d_{21}\|_2 = 1$, $dist(S_1, S_3) = \|d_{11}, d_{31}\|_2 = 1$, and $dist(S_2, S_3) = \|d_{21}, d_{31}\|_2 = \sqrt{2}$. Then for a given connectivity threshold $\delta = 1$, spatial set S_1 is connected to S_2 and S_3 according to Definition 5. The connected graph constructed from $\mathcal{S} = \{S_1, S_2, S_3\}$ is shown in Fig. 2(c), which satisfy $\forall N_i, N_j (i \neq j)$, there exists a path between N_i and N_j .

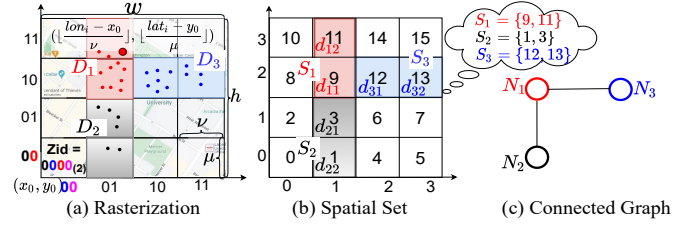


Fig. 2. Illustration of spatial set and connected graph.

3.2 Query Models

Definition 7. (Maximum Intersection Query (MIQ)) Given a collection of spatial sets $S^{\mathcal{D}} = \{S_1, S_2, \dots, S_{|S^{\mathcal{D}}|}\}$, a query set S_Q and a positive integer k , the MIQ aims to find a subset $\mathcal{S} \subseteq S^{\mathcal{D}}$ such that $|\mathcal{S}| \leq k$ and $\forall S_i \in \mathcal{S}$ and $\forall S_j \in S^{\mathcal{D}} \setminus \mathcal{S}$, it always satisfies $|S_Q \cap S_i| \geq |S_Q \cap S_j|$.

Definition 8. (Maximum Coverage Query with a Connection Constraint (MCQC)) Given a collection of spatial sets $S^{\mathcal{D}} = \{S_1, S_2, \dots, S_{|S^{\mathcal{D}}|}\}$, a query set S_Q and a positive integer k , the MCQC aims to find a subset $\mathcal{S} \subseteq S^{\mathcal{D}}$ such that $|\mathcal{S}| \leq k$, the graph constructed by \mathcal{S} and S_Q is a connected graph, and the number of elements contained by \mathcal{S} and S_Q is maximized:

$$\mathcal{S} = \arg \max_{\mathcal{S} \subseteq S^{\mathcal{D}}} |S_Q \cup (\cup_{S_i \in \mathcal{S}} S_i)|, \quad (2)$$

$$s.t. \quad |\mathcal{S}| \leq k,$$

\mathcal{S} and S_Q form a connected graph.

3.3 NP-Hardness of MCQC

Lemma 1. The maximum coverage query with a connection constraint is NP-hard.

Proof. To prove the NP-hardness of the MCQC, we show that any instance of the MCP can be reduced to an instance of the MCQC

in polynomial time. Considering a universe of elements $\mathcal{U} = \{u_1, u_2, \dots, u_n\}$ a collection of sets $\mathcal{A} = \{A_1, A_2, \dots, A_{|\mathcal{A}|}\}$ ($\forall A \in \mathcal{A}, A \subseteq \mathcal{U}$) and a positive integer k , the objective of the MCP is to find at most k subsets $\{A'_1, A'_2, \dots, A'_k\}$ such that $|\cup_{i=1}^k A'_i|$ is maximized. Given an arbitrary instance of the MCP, we sort the universe \mathcal{U} according to the lexicographic order, then create a mapping from the sorted universe $\mathcal{U} = \{u_1, u_2, \dots, u_n\}$ to a integer set $\{0, 1, \dots, n-1\}$. Then we can construct a $2^\theta \times 2^\theta$ grid in the space such that $2^\theta \times 2^\theta > n$. Since each cell in the grid can be represented by a unique integer ID, each element in \mathcal{U} can be mapped to a cell whose ID is equal to the integer. Thus, each set A_i in MCP can be represented as a spatial set S_{D_i} in MCQC, $\{n, n+1, \dots, 2^\theta \times 2^\theta - 1\}$ can be represented as the query set S_Q . We can see that the total reduction is performed in polynomial time. We set $\delta = 2^\theta \sqrt{2}$, then the connectivity constraint always satisfies since the distance between sets must be less than δ . Thus, the optimal solution for the MCQC instance must also be optimal for the corresponding MCP instance. The MCP has been proven to be NP-hard [27]. Therefore, if we can find the optimal solution for the MCQC instance in polynomial time, the MCP can be solved in polynomial time, which is not possible unless $P = NP$. Thus, the MCQC is NP-hard. \square

4 MSDS SEARCH FRAMEWORK

To support spatial dataset join and union searches simultaneously, we design a multi-source spatial dataset search framework. Unlike traditional distributed query framework, the MSDS contains a user interaction center and multiple independent data sources, as shown in Fig. 3. In MSDS, instead of transferring all datasets to the master computer for data partitioning, each data source organizes its data and constructs the local index. The center receives the distribution information from data sources and maintains a global index. All queries are sent to the center to search the global index and then forwarded to the corresponding data source for dataset search. The following provides a high-level description of index construction, as well as static and dynamic dataset searches.

Index Construction. We design the local and global indexes for data sources and interaction center. Instead of indexing each dataset, our global index is created by recording the distribution information of data sources, which is mainly used to filter out the data sources irrelevant to the query. Moreover, we propose a novel local index called the inverted-ball tree index, which effectively combines the features of both ball tree and inverted index while also supporting dynamic updates (see Section 5).

Static Dataset Search. We design static search algorithms to support efficient spatial join and union searches. When the interaction center receives a query request from a user, it first performs a global search and sends the query to the candidate data sources for local search. Combined with the index structure, we first design an efficient search algorithm based on the IBtree to solve the MIQ. For the NP-hard MCQC, we propose two heuristic algorithms to solve it (see Section 6).

Dynamic Dataset Search. To solve the problem of constantly updating the dataset, an intuitive approach is for the center to transmit the query to the data sources, and then each candidate source executes the top- k search. However, it is computationally expensive and incurs high communication costs. Therefore, we design a dynamic index updating strategy and an optimized search algorithm to maintain up-to-date top- k results (see Section 7).

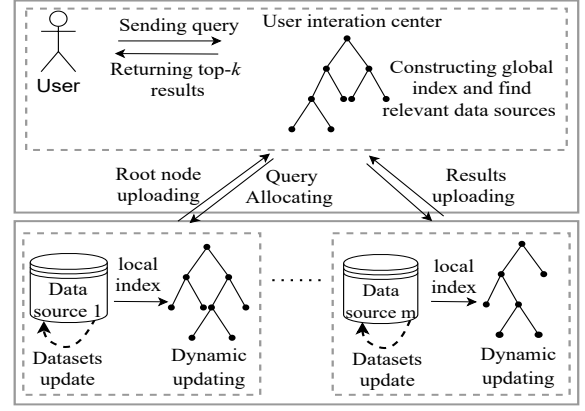


Fig. 3. The multi-source spatial dataset search framework.

5 INDEX CONSTRUCTION

5.1 Local Index Construction

In the following, we describe the process of building the local index. For each data source containing a collection of spatial datasets $\{D_1, D_2, \dots, D_m\}$, we devise an inverted-ball tree, called IBtree (see Fig. 4), to accelerate the MIQ and MCQC. Compared with the inverted and tree indexes, our IBtree can prune in batch those irrelevant spatial sets and quickly retrieve the candidate sets. For ease of understanding, we take a single data source as an example to illustrate the local index construction as below:

Example 3. As shown in Fig. 4, there are eight datasets in a data source. To create the local index, we first transform eight datasets into nodes and then build an IBtree in a top-down fashion by recursively dividing the spatial nodes into two groups.

When transforming spatial datasets into dataset nodes, each node should contain specific information about the spatial set. We present the formal definition of the dataset node, internal node, and leaf node in the index.

Definition 9. (Dataset Node) A dataset node $N_D = (id, rect, p, r, pa, s)$, where id is an identifier of the dataset, $rect$ is its minimum bounding rectangle (MBR), p is the pivot of the MBR, r is the radius of node, pa is the pointer address of the parent node, and s is the set representation of the spatial dataset.

Definition 10. (Internal Node) An internal node $N_I = (rect, p, r, ch, pa)$, where $rect$ is the MBR containing all child nodes, and ch is its child nodes. Note that the root node N_R and N_L have the same structure, but $N_R.pa$ is null.

Definition 11. (Leaf Node) A leaf node $N_L = (rect, p, r, ch, pa, inv)$, where inv is an inverted index of all the dataset nodes in the leaf node. inv contains posting lists that map the cell ID to a list of dataset ids that contain it.

In Algorithm 1, we show the whole process of IBtree index construction. Specifically, for a list of dataset nodes \mathcal{N} , we construct a new root node N_R that contains all dataset nodes as the root node (Line 2). If $N_R.size \geq f$, we choose the widest split dimension and divide the dataset nodes into two child lists based on their position in relation to the pivot of the new node (Lines 11 to 16). Then, we continue to build the sub-tree for each of the two child nodes (Lines 17 to 18). On the contrary, if the size of the nodes satisfies the leaf node capacity f , we create a leaf node N_L containing an inverted index (see Fig. 4).

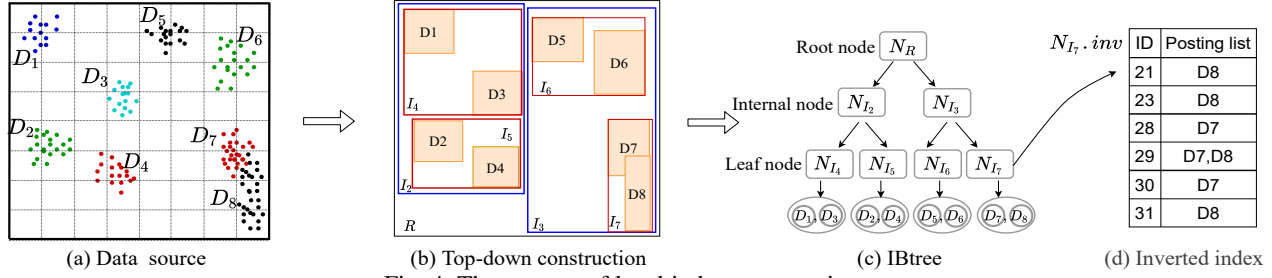


Fig. 4. The process of local index construction.

5.2 Global Index Construction

When the search scenario includes multiple data sources, one popular solution is to apply a traditional distributed framework with a master-slave structure [5, 21, 48]. It requires all datasets of slave nodes to be uploaded to the master, then the master node partition all datasets into equal chunks and stores them separately in the slave node to build indexes of the same setting, such as node capacity, resolution, etc. The partition information held by the master node serves as the global index. However, in our search scenario, each data source is independent. Thus, we propose a global index based on the local indexes, which not only plays the role of an “overview” index but is also suitable for situations where each data source builds its index in different settings.

The global index contains root nodes from local indexes and is used to send the query to candidate data sources. Thus, after the local index is built, each source sends its root node N_R to the center. Then, the center converts the pivot and MBR coordinates of N_R into latitude and longitude to resolve the situation where the resolution of the data source is different. Next, the center generates the global root node containing the region of all local root nodes and chooses a dimension to split it into two child sets until the global leaf node’s capacity is 1. The global index generation process is similar to building the local index, but there is no need to generate the inverted index for leaf nodes. The details of query filtering based on the global index are shown in Section 6.1.

Algorithm 1: $\text{IBtree}(\mathcal{N}, pa, f, d)$

Input: \mathcal{N} : a list of dataset nodes, pa : parent node, f : capacity, d : dimension
Output: N_R : the root node of IBtree

- 1 List of dataset nodes $\mathcal{N} \leftarrow \emptyset$;
- 2 $N_R \leftarrow$ generate the root node of \mathcal{N} ;
- 3 $N_R.\text{setParentNode}(pa)$;
- 4 **if** $N_R.\text{size} \leq f$ **then**
- 5 **foreach** $N_D \in \mathcal{N}$ **do**
- 6 $N_D.\text{setParentNode}(N_R)$;
- 7 $N_R.\text{addChildList}(N_D)$;
- 8 creating an inverted index for N_R ;
- 9 **else**
- 10 $\text{leftList}, \text{rightList} \leftarrow \emptyset$;
- 11 **foreach** $N_D \in \mathcal{N}$ **do**
- 12 $i \leftarrow$ pick a dimension;
- 13 **if** $N_D.\text{pivot}[i] \leq N_R.\text{pivot}[i]$ **then**
- 14 $\text{leftList.add}(N_D)$;
- 15 **else**
- 16 $\text{rightList.add}(N_D)$;
- 17 $N_R.\text{addLeftChild}(\text{IBtree}(\text{leftList}, N_R, f, i))$;
- 18 $N_R.\text{addRightChild}(\text{IBtree}(\text{rightList}, N_R, f, i))$;
- 19 **return** N_R ;

5.3 Dataset Graph Construction

To find the connected datasets in a data source \mathcal{D} and accelerate the MCQC search, we further design an auxiliary index: dataset

graph. The dataset graph $G(V, E)$ is an undirected graph that suffices: 1) each node $N_i \in V$ corresponds to a spatial set S_i ; 2) each edge $e(i, j)$ between N_i and N_j denotes two spatial sets S_i and S_j are connected, i.e., $\text{dist}(S_i, S_j) \leq \delta$; 3) the weight $w(i, j)$ on edge $e(i, j)$ denotes the number of sets intersections between S_i and S_j .

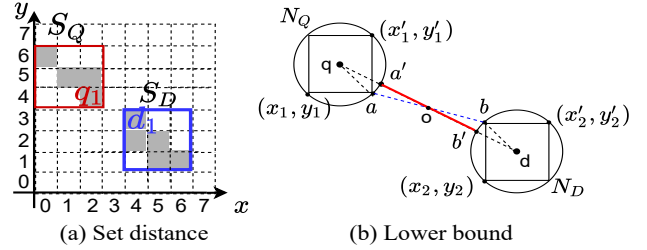


Fig. 5. Illustration of the distance between two spatial sets.

When constructing the dataset graph, it is expensive to compute the connectivity and intersection for each pair of datasets in the data source. Thus, we derive a lower bound on the distance based on the triangle inequality to accelerate the connectivity verification between two nodes.

Lemma 2. Let N_Q be a node of the query set S_Q , N_D be a node of the spatial set S_D . The lower bound of $\text{dist}(S_Q, S_D)$ is:

$$lb(N_Q, N_D) = \max\{\|N_Q.p, N_D.p\|_2 - N_Q.r - N_D.r, 0\}. \quad (3)$$

Proof. As we can see in Fig. 5, N_Q and N_D are two nodes transformed by spatial sets S_Q and S_D . Let a and b denote the two closest points in two MBRs, and a' and b' denote two intersect points in the line segment connected by two centers q and d . The triangle composed by points q, a and o is denoted by $\triangle qao$. According to the triangle inequality, we have:

$$\|q, a\|_2 + \|a, o\|_2 \geq \|q, o\|_2. \quad (4)$$

Next, based on Inequation (4), we can deduce that $\|a, o\|_2 \geq \|a', o\|_2$. Similarly, in $\triangle dbo$, we can deduce $\|b, o\|_2 \geq \|b', o\|_2$. Hence, $\|a, b\|_2 \geq \|a', b'\|_2$. As the set distance $\text{dist}(S_Q, S_D)$ is to find the minimum of the distance from an element in S_D to its nearest neighbor element in S_Q , $\text{dist}(S_Q, S_D) = \|a, b\|_2 \geq \|a', b'\|_2 = \max\{\|N_Q.p, N_D.p\|_2 - N_Q.r - N_D.r, 0\}$. \square

Example 4. As shown in Fig. 5, we can compute the set distance between the query set S_Q and the spatial set S_D is $\text{dist}(S_Q, S_D) = \|q_1, d_1\|_2 = \sqrt{5} \approx 2.236$. While based on Lemma 2, we can compute the lower bound of the set distance is $\max\{5 - \sqrt{2} - \sqrt{2}, 0\} \approx 2.172 \leq 2.236$, which proves the validity of Lemma 2.

We can filter out dataset nodes that cannot be connected with the query by combining Lemma 2 with IBtree to accelerate the dataset graph construction.

Example 5. As shown in Fig. 6, we consider a data source of eight spatial sets and the 1-connectivity constraint. Each spatial set is

represented as a node, the weight of which represents the number of cells occupied by the set. The weight of an edge represents the number of intersected cells between two sets.

Next, we show how to speed up the construction of the dataset graph based on the IBtree. Firstly, we initialize a graph $G(V, E)$, where V consists of all spatial dataset nodes $\{N_1, N_2, \dots, N_m\}$ in the data source. Then we traverse each node and add the undirected edge between N_i and N_j ($j \in [1, m]$ and $j \neq i$) until all nodes are visited. Specifically, for node N_1 , we perform a recursive search down the local index in which we can prune in batch those internal nodes whose MBR is disjoint with the query node to accelerate the search process. That is because if an internal node's MBR is disjoint with the query, there is no element in the set contained by the internal node that satisfies the distance from the element of the query set is less than or equal to 1.

After searching the index tree, we get all the candidate nodes that might be connected with the node N_1 . Then we verify the connectivity of each candidate node to N_1 . If $dist(S_1, S_j) \leq 1$, we add an undirected edge from N_1 to N_j and compute the number of intersected cells as the weight of the undirected edge. After traversing all the candidate nodes, we set the visit label of N_1 as true. Subsequently, we repeat the process for the next node in the data source. This process terminates until all nodes in the graph have been visited.

Although it appears to be expensive when constructing the dataset graph, the time complexity is actually greatly reduced with the help of local indexes. In practical applications, we can quickly find several candidate nodes based on the local index. Assuming that the maximum number of candidate nodes is a , the time complexity of constructing edges for a vertex in the dataset graph construction can be approximately $O(a \times n)$. Since the number of candidate nodes is much less than n after searching the IBtree, the time complexity is much less than $O(n^2)$.

6 STATIC DATASET SEARCH

In our scenario, the goal is to find joinable and unionable datasets with the query dataset. While the existing distributed queries mainly focus on the range query [5, 21], k-nearest neighbor (KNN) [6, 21], and all nearest neighbor (ANN) [40]. Thus, designing static dataset search algorithms to solve MIQ and MCQC is vital.

6.1 Query Distribution

Since the overall search process involves the communication between the data source and the interaction center, as well as the local search within the data source, communication cost and search efficiency are two main bottlenecks in our MSDS framework. Thus, we design two query distribution strategies to solve the above problems. The first strategy is to reduce the frequency of communication. Based on the global index, we can quickly find candidate data sources that may contain query results and only transfer the query request to them.

Specifically, when a query comes in, we recursively search the global index starting from the root node. For a tree node N_T , if $N_T.rect \cap N_Q.rect = \emptyset$ in MIQ or $lb(N_T, N_Q) \geq \delta$ in MCQC, we directly pruning it; otherwise, we perform the depth-first traversal on it until it is a leaf node. All leaf nodes that intersect with $N_Q.rect$ or may be connected to N_Q form the candidate sources. The interaction center only transmits the query

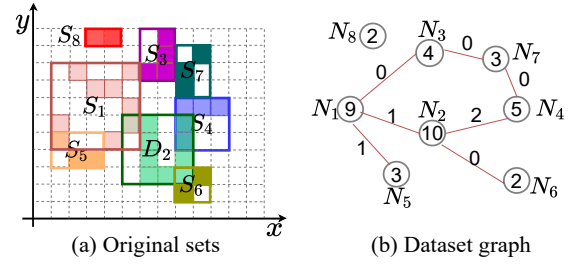


Fig. 6. Illustration of constructing the dataset graph.

to candidate sources, which reduces the communication cost of query distribution.

The second strategy is to reduce the number of bytes transferred during each communication between the interaction center and data sources. Because intersections only exist in the area where the MBR intersects, it is unnecessary to transmit the entire S_Q to each candidate source when performing the static search. The interaction center only transfers the portion of the query that has an MBR intersect to the candidate source to implement the local search to further reduce the communication cost.

6.2 Accelerating MIQ

The spatial dataset join search mainly focuses on the MIQ, that is, finding at most k datasets with the greatest number of intersections with the query. In this section, we propose a search algorithm based on the IBtree to accelerate the MIQ. The intersection number of two data sets whose MBR does not intersect is 0. Therefore, we can directly filter out those tree nodes that do not intersect with the query's MBR. For those nodes intersecting with the query node, we first propose an intersection upper bound based on the overlapping MBRs.

Lemma 3. (MBRBound) Let N_Q denote a query node with the set representation $S_Q = \{q_1, q_2, \dots, q_n\}$, N_L denote a leaf node containing multiple dataset nodes, and f denote the capacity of the leaf node, the intersection between N_Q and N_L is upper bounded by $\sum_{i=1}^n \phi(q_i)$,

$$\phi(q_i) = \begin{cases} 1, & \text{if } q_i \in (N_Q.rect \cap N_L.rect), \\ 0, & \text{otherwise} \end{cases}$$

where $N_Q.rect \cap N_L.rect$ denotes the intersection area between the MBRs of two nodes.

Proof. According to the MBRs of two nodes, we can easily compute the intersection region between two MBRs. As shown in Fig. 7, If a point $q_i \in S_Q$ is not in the intersection region, it cannot intersect with another set. On the contrary, if a point is in the intersection region, we count the number of ids that the query node falls in the intersection region. In Fig. 7(b), we can observe that the number falling in the intersection region is 2, which is the upper bound between N_Q and N_L . \square

However, from the above analysis, we can observe that the lower bound is difficult to estimate. Because even if the MBR of two datasets is completely overlapping, the distribution of cell IDs may be completely different. Thus, the lower bound based on the overlapping MBR is 0. To solve this problem, we propose lower and upper bounds based on the leaf node's posting list.

Lemma 4. (UpperBound) The upper bound of intersection between leaf node N_L and query node N_Q is $\sum_{i=1}^n \phi(q_i)\varphi(q_i)$.

$$\varphi(q_i) = \begin{cases} 1, & \text{if } q_i \in N_L.inv, \\ 0, & \text{otherwise} \end{cases}$$

where the definition of $\phi(q_i)$ is the same as in Lemma 3.

Proof. As shown in Fig. 7(c), for a cell ID q_i of N_Q falling into the overlapping MBR, if it is also stored by the key set of the leaf node, which indicates that at least one dataset intersects with N_Q . Therefore, the total number of cells that intersect with the key set of the inverted file is the upper bound between N_Q and N_L . \square

Lemma 5. (LowerBound) The lower bound of intersection between N_L and N_Q is $\sum_{i=1}^n \phi(q_i)\varphi(q_i)$.

$$\varphi(q_i) = \begin{cases} 1, & \text{if } q_i \in N_L.inv \& |q_i.pl| = f, \\ 0, & \text{otherwise} \end{cases}$$

where f is the capacity of the leaf node.

Proof. From Fig. 7(c) we can observe that the posting list of $N_L.inv$ stores the mapping from the cell ID to the spatial dataset. If the size of the $q_i.pl$ in $N_L.inv$ is equal to the leaf node's capacity $N_L.size$, then all dataset nodes contained by the leaf node must contain cell ID q_i . Therefore, the lower bound between the leaf node and the query node is the total number of cell IDs whose corresponding list size is equal to f . \square

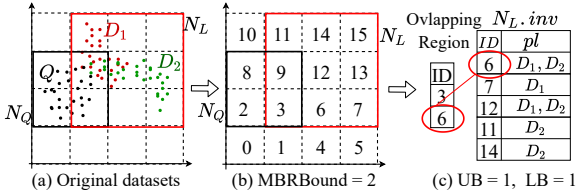


Fig. 7. Upper and lower bounds of the intersection of two nodes.

Based on the above lemmas, we propose a search algorithm based on the IBtree to accelerate the MIQ. Algorithm 2 shows the process of the algorithm. Firstly, based on the BranchAndBound Function, we can directly prune in batch those nodes whose MBRs are not intersected with the query's MBR because their set intersection must be 0 (Lines 25 to 27). Then, for each intersected leaf nodes N_R , if the upper bound of N_R is greater than the current lower bound in the priority queue, it will become a candidate leaf node (Lines 17 to 23).

After obtaining the first-round candidate nodes, we traverse each candidate leaf node N_L and compute the set intersection by scanning the posting lists of N_L . When the number of result set $\mathcal{R}.size < k$, the candidate dataset is directly inserted into \mathcal{R} ; otherwise, we compare the set intersection of each candidate dataset with the k -th largest value in \mathcal{R} and judge whether to insert it into \mathcal{R} . Finally, we can obtain the result set \mathcal{R} . (Lines 3 to 12).

6.3 Accelerating MCQC

As we illustrate in Example 1, spatial dataset union search aims to find k spatial datasets that are connected and have the maximum coverage. To achieve this goal, we propose a novel MCQC (see Definition 8) to support the spatial union search, which is a variant of the classic *MCP*. An exact algorithm for MCQC is to traverse all possible combinations of k sets from $\mathcal{S}^D = \{S_1, S_2, \dots, S_m\}$, \mathcal{C}_m^k in total, to find the connected combination with the maximum coverage. However, when n is large, computing all possible combinations becomes computationally slow. Therefore, we develop a greedy approach based on the local index to solve the MCQC.

The strategy of our greedy algorithm is to iteratively pick the set that is connected to the query and has the maximum number of uncovered sets. Thus, we denote the increment function of set

Algorithm 2: IBtreeSearch(N_R, N_Q, k)

Input: N_R : root node of local index, N_Q : query node, k : number of results

Output: \mathcal{R} : result queue

```

1 PQ, R ← Initialize two priority queues;
2 BranchAndBound( $N_R, N_Q, PQ$ );
3 foreach  $N_L \in PQ$  do
4   Compute the exact intersection of all nodes contained by
    $N_L$  with  $N_Q$  according to  $N_L.inv$ ;
5   foreach  $N_D \in N_L$  do
6     if  $\mathcal{R}.size \leq k$  then
7        $\mathcal{R}.Insert(N_D)$ ;
8     else
9       if  $|N_D \cap N_Q| > \mathcal{R}.peek()$  then
10         $\mathcal{R}.Dequeue()$ ;
11         $\mathcal{R}.Insert(N_D)$ ;
12 return  $\mathcal{R}$ ;

```

Function BranchAndBound(N_T, N_Q, PQ):

Input: N_T : tree node, N_Q : query node, PQ : priority queue;

```

14 maxUB ←  $-\infty$ , maxLB ←  $+\infty$ ;
15 if  $N_T$  is leaf node then
16   if  $overlap(N_T.rect, N_Q.rect)$  then
17      $N_T.lb, N_T.ub$  ← Compute the lower and upper
     bounds based on the Lemmas 4 and 5;
18   if  $PQ.isEmpty()$  then
19      $PQ.Insert(N_T)$ ;
20   if  $N_T.ub > PQ.head().lb$  then
21     while  $N_T.lb \geq PQ.head().ub$  do
22        $PQ.Dequeue()$ ;
23        $PQ.Insert(N_T)$ ;
24 else
25   if  $overlap(N_T.rect, N_Q.rect)$  then
26     BranchAndBound( $N_T.leftChild, N_Q, C$ );
27     BranchAndBound( $N_T.rightChild, N_Q, C$ );

```

coverage as g , which represents the increase in the number of sets after picking the spatial set S_D into the current result set \mathcal{R} :

$$g(S_D, \mathcal{R}) = |S_D \cup (\cup_{S_i \in \mathcal{R}} S_i)| - |\cup_{S_i \in \mathcal{R}} S_i|. \quad (5)$$

6.3.1 Greedy Algorithm with Spatial Merge (GASM)

To solve the MCQC effectively, we first design a greedy algorithm with space merging by combining the IBtree with the greedy strategy. Algorithm 3 shows the concrete process of GASM, where we first initialize a result set \mathcal{R} and put query node N_Q into it. Next, we perform k depth-first search in the IBtree and find the spatial set $S_D \in (\mathcal{S}^D \setminus \mathcal{R})$ that is connected to the merged set $S_M = \cup_{S_i \in \mathcal{R}} S_i$ and has the maximum coverage increment $g(S_D, \mathcal{R})$ in each iteration.

In each search process, we can quickly obtain all candidate leaf nodes that may satisfy the connectivity constraint based on Lemma 2 and IBtree. (Lines 15 to 21). Then for each candidate leaf node, we can decide whether to filter based on the maximum increment it can bring. Since the inverted index of each leaf node $N_L.inv$ records cell IDs of all dataset nodes it contains, $\forall N_D \in N_L$, the number of cells $N_D.size \leq N_L.inv.size$. In each round of searching, we use a symbol τ to represent the increment value of the local optimal set found so far. Then $N_L.inv.size \leq \tau$ means all dataset nodes contained by the N_L cannot be an local optimal set. Thus, this leaf node can be filtered safely; otherwise, we compute the exact number of coverage of each dataset node using the inverted index and judge whether it is the local optimal set (Lines 5 to 10).

By repeating this step until the whole candidate set is traversed, we can add the set that satisfies the connectivity and has

Algorithm 3: $\text{GASM}(N_R, N_Q, \delta, k)$

Input: N_R : root node of local index, N_Q : query node, δ : connectivity threshold, k : number of results

Output: \mathcal{R} : result set

```

1  $C \leftarrow \emptyset, \mathcal{R} \leftarrow \{N_Q\}, N_M \leftarrow N_Q;$ 
2 while  $\mathcal{R}.size() \leq k$  do
3    $\tau \leftarrow -\infty, N_{best} \leftarrow null;$ 
4    $\text{FindConnectSet}(N_R, N_M, \delta, C);$ 
5   foreach  $N_L \in C$  do
6     if  $N_L.inv.size > \tau$  then
7       foreach  $N_D \in N_L.ch$  do
8         if  $g(N_D, \mathcal{R}) > \tau$  then
9            $N_{best} \leftarrow N_D;$ 
10           $\tau \leftarrow g(N_D, \mathcal{R});$ 
11    $\mathcal{R}.add(N_{best});$ 
12    $N_M \leftarrow \text{Merge } N_M \text{ and } N_{best};$ 
13 return  $\mathcal{R};$ 

```

```

Function  $\text{FindConnectSet}(N_T, N_Q, \delta, C)$ :
Input:  $N_T$ : tree node,  $N_Q$ : query node,  $\delta$ : connectivity
threshold,  $C$ : candidate leaf nodes;
15  $lb \leftarrow ||N_R.p, N_Q.p||_2 - N_R.r - N_Q.r;$ 
16 if  $lb < \delta$  then
17   if  $N_T$  is leaf node then
18      $C.add(N_T);$ 
19   else
20      $\text{FindConnectSet}(N_T.leftChild, N_Q, \delta, C);$ 
21      $\text{FindConnectSet}(N_T.rightChild, N_Q, \delta, C);$ 

```

the maximum increment to \mathcal{R} . In the next iteration, we generate a new node N_M with a larger MBR by merging the existing sets in \mathcal{R} . Then we treat the new node as a query and repeat the search process to find the next set. After k iterations, the algorithm terminates.

6.3.2 Greedy Algorithm based on Dataset Graph (GADG)

The above greedy algorithm requires iterating k times in the IBtree to find a heuristic solution, which is time-consuming. Thus, we propose another Greedy Algorithm based on the Dataset Graph, called GADG, to further accelerate the MCQC. As we introduced in Section 5.2, the connectivity information and the number of intersected cells between all datasets are pre-computed and stored in the dataset graph. When a query arrives, we only need to find the local optimal spatial datasets from the data source based on the IBtree in the first iteration. Then, we can obtain the maximum coverage set by accessing the connected edge of the result set in the dataset graph in the following search process without traversing the IBtree repeatedly. Thus, this approach can generate the same solution as GASM but requires only one search on the local index, significantly accelerating the search process.

Example 6. We show how to use the dataset graph to quickly find the greedy solution in Fig. 8. Given a query node N_Q , we first initialize a result set \mathcal{R} to record the solution and add N_Q to \mathcal{R} . We then first implement the depth-first search in the local index tree and obtain all connected edges and the set intersections with the query node. We traverse the edges associated with N_Q , find the node N_2 that has the maximum coverage, and add N_2 to the result \mathcal{R} , as shown in Fig. 8(a). Next, we find new nodes with maximum coverage for each node in \mathcal{R} and select the best one from them to add to \mathcal{R} . We can see that N_1 has the maximum coverage $9 - 1 = 8$ corresponding to N_2 , whereas N_5 has the maximum coverage $3 - 0 = 3$ corresponding to Q . Since $8 > 3$, we add N_1 to \mathcal{R} as shown in Fig. 8(b). This step repeats until the

number of nodes in the result set is equal to $k + 1$. Fig. 8(c) shows the top-3 results generated by the GADG algorithm.

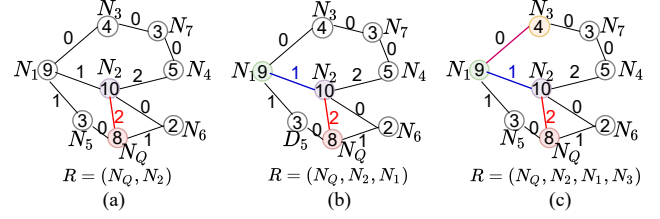


Fig. 8. Illustration of the GADG algorithm.

6.3.3 Approximation Guarantee

Next, we provide the approximation guarantee, which indicates our greedy algorithms achieve $(1-1/e)$ -approximation under the condition that at the start of each iteration, the current result set can connect with at least one set in the optimal solution and the gain brought by the set is above the average value of all the gains brought by the optimal solution. The analysis of the approximation guarantee is as follows. First, as shown in Table 1, S_Q denotes the query set, $\mathcal{S}^D = \{S_1, S_2, \dots, S_m\}$ denotes a collection composed of m spatial sets.

Let $U = (\cup_{i=1}^m S_i) \cup S_Q$ be the set of all set elements, $\mathcal{R} = \{S_Q, S'_1, \dots, S'_k\}$ denotes the output of result set after k iterations in our Algorithm 3. $C_i = (\cup_{j=1}^i S'_j) \cup S_Q$ denote the set of elements covered by the end of iteration i , and $V = U - C_{i-1}$ denotes the set of elements which are not in C_{i-1} . Let the optimal solution be $\{S_Q, S_1^*, \dots, S_k^*\}$ and $CS_k = \cup_{j=1}^k S_j^*$. Then we present Lemma 6,

Lemma 6. At the start of each iteration i , if the C_{i-1} is connected with at least one optimal set $S^* \in \{S_1^*, \dots, S_k^*\}$, where $|S^* \cap V| \geq \frac{1}{k} \sum_{j=1}^k |S_j^* \cap V|$, then we have

$$|S'_i \cap V| = |C_i| - |C_{i-1}| \geq \frac{|OPT| - |C_{i-1}|}{k}. \quad (6)$$

Proof. Let OPT is the union of CS_k and S_Q , i.e., $OPT = CS_k \cup S_Q$, $|OPT|$ denotes the number of elements in OPT . Thus, at the start of iteration i , the number of elements covered in OPT but not in C_{i-1} is

$$|OPT - C_{i-1}| = |OPT| - |OPT \cap C_{i-1}| \geq |OPT| - |C_{i-1}|. \quad (7)$$

Moreover, $|(CS_k \cup S_Q) \cap V|$ is equal to $|OPT - C_{i-1}|$, that is

$$\begin{aligned} |(CS_k \cup S_Q) \cap V| &= |OPT \cap V| \\ &= |OPT \cap (U - C_{i-1})| \\ &= |(OPT \cap U) - (OPT \cap C_{i-1})| \\ &= |OPT| - |(OPT \cap C_{i-1})| \\ &= |OPT - C_{i-1}|. \end{aligned} \quad (8)$$

Therefore, we obtain that

$$|(CS_k \cup S_Q) \cap V| \geq |OPT| - |C_{i-1}|. \quad (9)$$

In addition, we also have

$$\begin{aligned} |(CS_k \cup S_Q) \cap V| &= |(CS_k \cap V) \cup (S_Q \cap V)| \\ &= |(CS_k \cap V)|. \end{aligned} \quad (10)$$

Then we derive that

$$|(CS_k \cap V)| \geq |OPT| - |C_{i-1}|. \quad (11)$$

Dividing the two sides of Inequality (11) by k , we obtain that

$$\begin{aligned} \frac{|(CS_k \cap V)|}{k} &= \frac{|(\cup_{j=1}^k S_j^*) \cap V|}{k} \\ &= \frac{|\cup_{j=1}^k (S_j^* \cap V)|}{k} \\ &\geq \frac{|OPT| - |C_{i-1}|}{k}. \end{aligned} \quad (12)$$

We know that

$$\sum_{j=1}^k |S_j^* \cap V| \geq |\cup_{j=1}^k (S_j^* \cap V)|. \quad (13)$$

By Inequalities 12 and 13, we obtain that

$$\frac{\sum_{j=1}^k |S_j^* \cap V|}{k} \geq \frac{|\cup_{j=1}^k (S_j^* \cap V)|}{k} \geq \frac{|OPT| - |C_{i-1}|}{k}. \quad (14)$$

We know that at least one optimal set $S^* \in \{S_1^*, \dots, S_k^*\}$ is connected with C_{i-1} , where

$$|S^* \cap V| \geq \frac{\sum_{j=1}^k |S_j^* \cap V|}{k}. \quad (15)$$

Combining Inequalities 14 and 15, we obtain that

$$|S^* \cap V| \geq \frac{|OPT| - |C_{i-1}|}{k}. \quad (16)$$

In addition, based on Lines 5 to 11 of Algorithm 3, we find the spatial set S'_i with the maximum coverage increment in the iteration i . That is

$$|S'_i \cap V| \geq |S^* \cap V|. \quad (17)$$

Thus, by Inequalities 16 and 17, we conclude that: for all $i \in \{1, 2, \dots, k\}$,

$$|S'_i \cap V| = |C_i| - |C_{i-1}| \geq |S^* \cap V| \geq \frac{|OPT| - |C_{i-1}|}{k}. \quad (18)$$

Lemma 7. For all $i \in \{1, 2, \dots, k\}$, $|C_i| \geq \frac{|OPT|}{k} \sum_{j=0}^{i-1} (1 - 1/k)^j + (1 - 1/k)^i |S_Q|$.

Proof. We use induction to prove the correctness of Lemma 7. For convenience, we let $o = |OPT|/k$ and $t = (1 - 1/k)$. At the start of our algorithm, the set of covered elements can be considered as S_Q , i.e. $C_0 = S_Q$. Firstly, the base case $i = 1$ is trivial as the first choice $|C_1|$ has at least $\frac{|OPT|}{k} + (1 - 1/k)|S_Q|$ elements by Lemma 6. Then we suppose inductive step i holds, and prove that it holds for $i + 1$. By Lemma 6, we obtain that

$$\begin{aligned} |C_{i+1}| &\geq |C_i| + \frac{|OPT| - |C_i|}{k} \\ &= o + t|C_i| \\ &\geq o + t(o \sum_{j=0}^{i-1} t^j + t^i |S_Q|) \\ &= ot^0 + o \sum_{j=1}^i t^j + t^{i+1} |S_Q| \\ &= o \sum_{j=0}^i t^j + t^{i+1} |S_Q| \\ &= \frac{|OPT|}{k} \sum_{j=0}^i (1 - 1/k)^j + (1 - 1/k)^{i+1} |S_Q|. \end{aligned} \quad (19)$$

The first inequality is by Lemma 6, and the last inequality is from inductive hypothesis. \square

Finally, we have the following theorem and prove it.

Theorem 1. At the start of each iteration i , if the C_{i-1} is connected with at least one optimal set $S^* \in \{S_1^*, \dots, S_k^*\}$, where $|S^* \cap V| \geq \frac{1}{k} \sum_{j=1}^k |S_j^* \cap V|$, then Algorithm 3 is a $(1-1/e)$ -approximation algorithm for MCQC.

Proof. Based on Lemma 7, we obtain that

$$\begin{aligned} |C_k| &\geq \frac{|OPT|}{k} \sum_{j=0}^{k-1} (1 - 1/k)^j + (1 - 1/k)^k |S_Q| \\ &= \frac{|OPT|}{k} \times \frac{1 - (1 - 1/k)^k}{1 - (1 - 1/k)} + (1 - 1/k)^k |S_Q| \\ &= |OPT|(1 - (1 - 1/k)^k) + (1 - 1/k)^k |S_Q| \\ &\geq |OPT|(1 - (1 - 1/k)^k). \end{aligned} \quad (20)$$

Moreover, we know that $1 + x \leq e^x$ for all $x \in \mathbb{R}$, which means $(1 - 1/k)^k \leq (e^{-1/k})^k = 1/e$. Then $1 - (1 - 1/k)^k \geq 1 - 1/e$. Thus, we can derive that

$$|C_k| \geq (1 - 1/e)|OPT|, \quad (21)$$

which proves that our greedy algorithm provides a $(1-1/e)$ -approximation. \square

7 DYNAMIC DATASET SEARCH

7.1 Dynamic Index Updating

As described in Section 5.1, our local index is a bidirectional pointer structure, where each dataset node N_D not only contains the pointer of child nodes $N_D.ch$ but also contains the pointer of parent node $N_D.pa$. Thus it can quickly support dynamic updates without rebuilding the index every time the dataset is updated.

7.1.1 Updating Local Index

There are two common types of data updates in the data source: one is the update of existing datasets, and the other is the insertion of new datasets. To update a dataset, we can find the original dataset node in the tree in $O(1)$ according to the unique dataset $N_D.id$. Subsequently, we replace the original node N_D with the updated dataset node N'_D and iteratively update $(rect, p, r, ch, pa)$ of the parent node from the bottom up until the parent node contains the child node completely.

To insert a new dataset D into the IBtree, we first find the node N_I with the minimum distance $\|N_I.p, N_D.p\|_2$ in each layer of the tree, and recursively update the node information. When the tree node is a leaf node, we insert N_D into the leaf node. However, it should be noted that if the leaf node capacity is greater than the predetermined leaf node capacity, we need to split the node.

7.1.2 Updating Dataset Graph

When a spatial dataset D is updated, the corresponding dataset graph G should also be updated. Specifically, we find all nodes connected to N_D based on the IBtree and compute the set intersection. We then update the weight on the original edges and add undirected edges between the updated node and new nodes in G . Similarly, when adding a new spatial dataset D in the dataset graph, we need to find all connected nodes with N_D in the same way and add undirected edges and weight between them.

7.2 Top- k Dynamic Search

Dynamic search, which aims to maintain the up-to-date top- k search results, is becoming an inevitable search model due to the need for instant replies to queries on spatial datasets updating over time. The existing studies mainly focus on building an index for a stream of queries [15, 16, 30, 44]. However, quickly perceiving the change in query results and communicate with the interaction center is critical when datasets are updated in batches. To solve the

above problem, we design a dynamic search strategy based on the index structure (Section 5) for MIQ and MCQC simultaneously.

In the MIQ with a set of data stream updates, for an updated dataset D , we check if $N_D.rect \cap N_Q.rect = \emptyset$. If not, the source can directly filter out the updated set D and continues to process the next data stream; otherwise, we compute the lower and upper bounds according to Lemmas 4 and 5 and compare the boundary with the current k -th results. While in the MCQC with a set of data stream updates, we need to check if $dist(N_D, N_Q) \leq \delta$ and the upper bound of coverage is greater than the current k -th results. For those unfiltered datasets, we need to verify the connectivity between N_Q and N_D and compute the exact value of coverage. Only when the result set is updated, we transfer the new result to the interaction center; otherwise, we will not communicate with the interaction center to avoid invalid transmission costs.

8 EXPERIMENTS

We first introduce the experimental settings in Section 8.1. Then we evaluate the efficiency of constructing the IBtree and dataset graph in Section 8.2. Next, we present the search performance and communication cost of the MIQ in Section 8.3 and the MCQC in Section 8.4 on five real-world spatial data sources.

8.1 Experimental Setups

8.1.1 Datasets

We conduct experiments on the following five data sources, each of which is downloaded from an open-source spatial data portal. Fig. 9 presents the dataset distribution heatmaps, showing the density of spatial datasets in the space.

- Baidu-dataset¹ is collected from the Baidu Maps Open Platform, which contains spatial datasets from different industry categories for 28 cities in China.
- BTAA-dataset² is collected from the Big Ten Academic Alliance Geoportal, which contains spatial data for the mid-western US, such as Illinois, Indiana, Michigan, and others.
- NYU-dataset³ is collected from the NYU Spatial Data Repository, which contains geographic information on multiple subjects like census and transportation worldwide.
- Transit-dataset⁴ is collected from Big Geoportal, which contains different kinds of transportation data from Maryland and Washington D.C., such as buses, metro, and waterways.
- UMN-dataset⁵ is collected from the Data Repository for the University of Minnesota, which contains geographic information from various topics like agriculture, ecology, and city.

8.1.2 Environment

We conducted all experiments on six devices equipped with a 2.90 GHz Intel(R) Core(TM) i5-12400 processor and 16GB of memory, wherein one device serves as the interaction center and the other five as data sources in different locations to perform local searches. The implementation code can be obtained from the anonymous GitHub repository⁶.

1. <https://lbsyun.baidu.com/>
 2. <https://geo.btaa.org/>
 3. <https://geo.nyu.edu/>
 4. <https://geo.btaa.org/>
 5. <https://conservancy.umn.edu/drum>
 6. https://github.com/yangwenzhe/MSDS_code

TABLE 2: Parameter settings.

Parameter	Settings
k : number of results	{ <u>10</u> , 20, 30, 40, 50}
n : number of queries	{ <u>10</u> , 20, 30, 40, 50}
θ : resolution	{10, 11, <u>12</u> , 13, 14}
δ : connectivity	{0, <u>5</u> , 10, 15, 20}
f : leaf node capacity	{ <u>10</u> , 100, 200, 300, 400}
β : number of datasets updates	{100, 150, 200, 250, 300}

8.1.3 Query and Parameter Generation

We randomly select 50 datasets from all downloaded datasets as the query datasets. We alter several key parameters including k , n , θ , δ , f and β to observe the experimental results. Firstly, the parameter θ determines the grid’s size; thus, we set the resolution according to the distance sampling [41]. For example, one degree of longitude or latitude is about 111km. If we divide the globe into a $2^{12} \times 2^{12}$ grid, then each cell’s area is about $10km \times 5km$. Similarity, the δ can be set according to the closest distance between the point pairs of two spatial datasets that the user requires. For other parameters, we can also set them according to the requirements of users and data sources. We summarize the parameter settings in Table 2. To control variables, when we study the effect of a change in one of the parameters, we use the default settings for the other parameters, which are underlined in Table 2.

8.2 Efficiency of Index Construction

To accelerate the search performance of MIQ and MCQC, we design two index structures IBtree and dataset graph. Thus, we first show the index construction performance of the IBtree and dataset graph in Figs. 10 and 11. Since the IBtree combines the characteristics of tree index and inverted index, we choose two classical tree indexes and two inverted indexes for comparison.

- QuadTree [23]: QuadTree mainly divides the spatial points by dividing the whole space into four quadrants recursively.
- Rtree [24]: Rtree is to group nearby datasets and represent them with their MBR in the next level of tree.
- STS3 [34]: STS3 divides the plane into cells and constructs an inverted index to accelerate the intersection computation.
- Josie [52]: Josie designs a sorted inverted index where each posting list contains the id, position, and the size of datasets.

Comparison of Several Indexes. We compare the index construction time of the IBtree and four indexes as the resolution increases, as shown in Fig. 10. Firstly, we can observe that STS3 is the fastest at lower resolutions. However, as θ increases, IBtree becomes faster than STS3. This is because when the θ is small, the size of each spatial set is small. Compared to STS3’s inverted index, IBtree takes extra tree index building time, as the inverted index needs to be built for each leaf node. But as the θ increases, the size of each spatial set becomes larger. The size of the posting lists in STS3’s inverted index becomes larger. As a result, it takes more time to traverse the posting list and insert data into it.

Next, we can observe that the QuadTree is slower than IBtree and Rtree in most cases. The reason is that the QuadTree is built by inserting the cell coordinates of each spatial set one by one into the tree index, while the Rtree and IBtree are built based on the MBR of each spatial set. However, when the scale of data source is small, such as Transit, QuadTree is faster than Rtree. In addition, we also can observe that the IBtree is always slightly faster than Rtree. This is because the Rtree is a balanced search tree, which needs more time to organize the spatial datasets’ MBR. We can also see that the Josie is slower than the other four algorithms

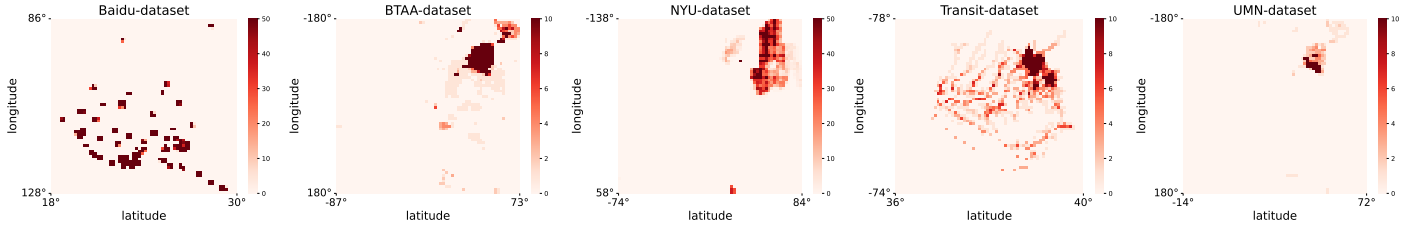


Fig. 9. The heatmaps of five data sources.

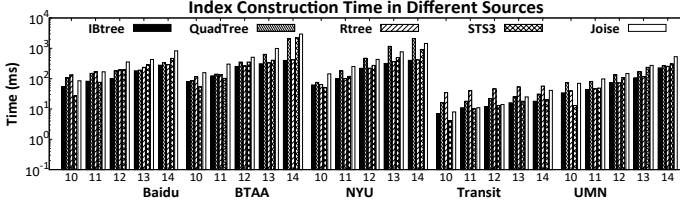


Fig. 10. IBtree Index construction time in MIQ.

in most cases. This is because Josie takes more time to insert the spatial set element into the posting list in sorted order.

Efficiency of Dataset Graph. When performing MCQC, we can quickly generate the dataset graph with the help of IBtree on the first search. Then we can serialize the dataset graph, and next time we can get it quickly by de-serialization without having to build it again. Fig. 11 shows the time of generating and loading the dataset graph. We can see that the dataset graphs’ construction can be completed in several hundred milliseconds, which shows the acceleration provided by the IBtree index is very effective. In addition, we can observe that as the θ increases, the time to generate the dataset graph gradually increases, while the time to load the dataset decreases gradually. The reason is that when θ is small, the size of each spatial set is smaller, and the computation of connectivity and edge weights is faster, whereas the opposite is true when θ is large. However, when loading the dataset graph, a smaller θ will result in more spatial sets satisfying the connectivity constraint and more edges in the dataset graph, so it will take more time to reconstruct the dataset graph through de-serialization.

8.3 Efficiency of MIQ Search and Communication

8.3.1 Efficiency of Top- k Search

We compare MSDS with four algorithms based on the indexes introduced in Section 8.2. Specifically, when performing MIQ based on the QuadTree, we find all leaf nodes that intersect the query dataset and record the dataset ID of each intersecting node. In addition, when performing MIQ based on the Rtree, we find all intersecting datasets based on their MBR, then compute the set intersection number. For STS3 and Josie, we directly apply them to spatial sets to compute set intersection.

Effect of Number of Results. From Fig. 12, we can see that the MSDS achieves the best search performance over the other four algorithms, indicating that our index and pruning strategies are effective. Although Rtree and QuadTree also apply the tree index, Rtree achieves the second-best performance compared with QuadTree, as the QuadTree is constructed based on all spatial points of all datasets, we need to find all set elements that intersect with the query and record the sorted results, which is similar to the inverted index. For two algorithms based on the inverted index, we can see that Josie runs faster than STS3 because Josie’s posting list contains the location and number of sets except for the dataset id, which can terminate the search early by the prefix filter.

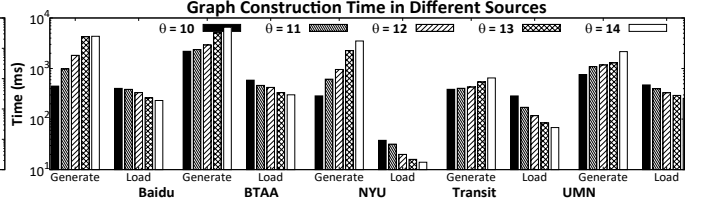


Fig. 11. Dataset graph construction time in MCQC.

Effect of Resolutions. We increase θ to investigate the search performance of our algorithms compared with the other four algorithms. From Fig. 13, we can observe that the search time of the five algorithms increases gradually as the θ increases. The reason is that each spatial dataset is divided into finer granularity as the θ increases. However, the MSDS is always faster than the other four algorithms under different resolutions. The reason is that our algorithm can quickly filter out unpromising leaf nodes using the IBtree and bounds. In addition, we can also see that the two algorithms based on the tree index maintain a better search performance than the other two based on the inverted index, indicating that filtering based on the geographic characteristics of the spatial dataset can provide better search performance.

Effect of Number of Queries. Fig. 14 shows the search performance as the number of queries increases. We can see that the search time of MSDS and Rtree increase slightly. The running time at $n = 50$ increases only by about 3 compared to the running time at $n = 10$. While the other four algorithms have an increase of 4 or more. The reason is that the search based on the tree index has a faster filtering power than the other three algorithms, so it can show more stable search performance as the number of queries increases. In addition, the search based on the QuadTree is to find the intersection point, which is similar to the inverted index, thus it has a slower time than the other two tree algorithms.

Effect of Node Capacities. We also investigate the search performance when increasing leaf nodes’ capacity f , and the results are shown in Fig. 15. Here, we only show the experiment results of MSDS and Rtree, as the leaf node capacity in QuadTree is 4, STS3 and Josie are based on inverted index. We can observe that the running time of MSDS increases slightly as the f increases. This is because bigger leaf nodes cannot be pruned easily, which degrades the performance. However, our algorithm still has a better performance than the Rtree, as our algorithm has a stronger filtering power and faster computation time based on the bound.

8.3.2 Efficiency of Communication

We compare the communication cost of performing the MIQ when spatial datasets are updated. MSDS applied the dynamic search algorithm proposed in Section 7, whereas the other four comparison algorithms use the static search.

Communication Cost and Transmission Time. Fig. 16 shows the number of bytes transferred. We can see that the number of bytes transferred by five algorithms gradually increases as the

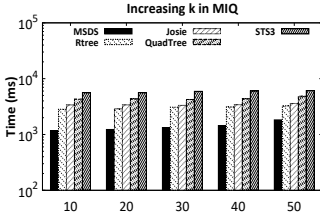


Fig. 12. Top- k search time with the increase of k .

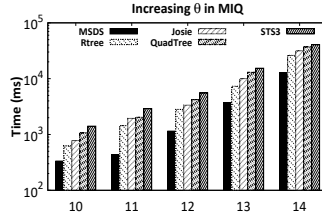


Fig. 13. Top- k search time with the increase of θ .

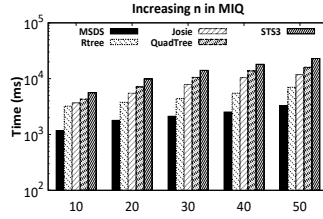


Fig. 14. Top- k search time with the increase of n .

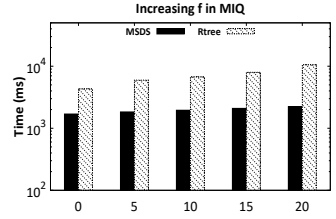


Fig. 15. Top- k search time with the increase of f .

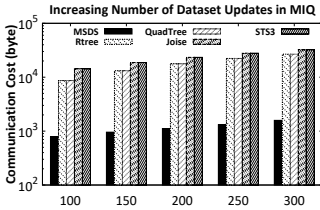


Fig. 16. Communication cost with the increase of updates.

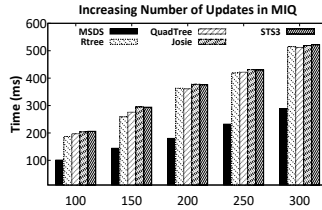


Fig. 17. Transmission time with the increase of updates.

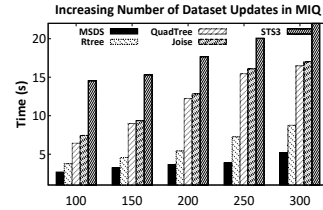


Fig. 18. Search time with the increase of updates.

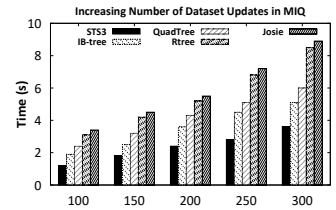


Fig. 19. Index updating time with the increase of updates.

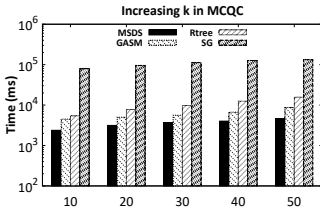


Fig. 20. Top- k search time with the increase of k .

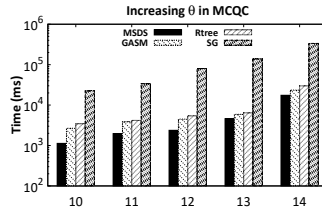


Fig. 21. Top- k search time with the increase of θ .

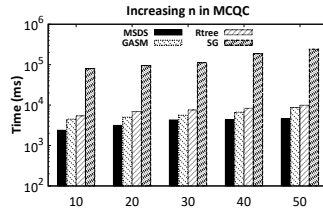


Fig. 22. Top- k search time with the increase of n .

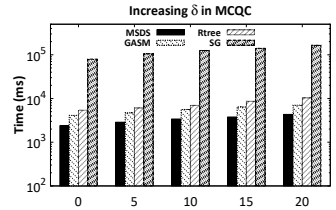


Fig. 23. Top- k search time with the increase of δ .

β increases, wherein the MSDS transmits the fewest bytes. This is because the MSDS only transmits the query request once and returns updated results only when changes occur in the result set. However, in the other four algorithms, we need to re-perform the search after each update to the dataset, which involves multiple transmissions of the query and result set. In addition, Rtree and QuadTree transmit slightly fewer bytes than Josie and STS3, as they can build global indexes based on the local root node and only send queries to candidate data sources. Fig. 17 shows the transmission time in dataset search. Since the transmission time is inversely proportional to the network bandwidth when the network bandwidth is constant, the more bytes that are transmitted, the longer the transmission time will be.

Search and Index Update Time. We also compare the search time of the five algorithms as the number of dataset updates β increases. From Fig. 18 we can see that the dynamic search strategy of MSDS can effectively improve search efficiency, and the advantages gradually increase with the increase of β . In addition, Fig. 19 shows the index dynamic updating time with the increase of β . We observe that the index updating of IBtree is slower than STS3 but faster than the others. This is because compared with STS3, we need to update the tree structure according to the node insertion or updating strategies described in Section 7. However, since the IBtree is a bidirectional pointer structure, it is faster in inserting and deleting than QuadTree and Rtree. In addition, we can also see that Josie's index updating is consistently slower than the other algorithms. This is because Josie takes more time in sorting the elements in each set and inserting the dataset into the posting list in a sorted order.

8.4 Efficiency of MCQC Search and Communication

8.4.1 Efficiency of Top- k MCQC

In MCQC, we vary key parameters k , θ , n and δ to evaluate the experimental results of MSDS and the following algorithms.

- SG [27]: It is a standard greedy algorithm for solving classic MCP. Here, we modify the SG to consider the connectivity constraint, that is, we traverse all sets in the data source and find the spatial set that is connected with the query and covers the maximum number of sets at each iteration. The SG does not use the index to speed up the search process.
- GASM: It is a variant of our MSDS, which uses the IBtree index and GASM search algorithm to solve the MCQC.
- MSDS: MSDS combines the IBtree, dataset graph, and heuristic algorithm GADG to accelerate the MCQC search.
- Rtree: Rtree uses the Rtree and GASM search algorithm to solve the MCQC.

Effect of Number of Results. Fig. 20 shows the search time of three algorithms with the increase of k . We observe that MSDS performs better than the other two greedy algorithms. Because the MSDS only needs to search in the index tree once to find the node connected with the query. Then it can directly find the node with the maximum coverage according to the dataset graph, significantly reducing the search time. In addition, we can see that GASM is slightly faster than Rtree, which indicates our IBtree index is more efficient in solving the MCQC. The SG is significantly slower than the other three algorithms. The main reason is that the SG needs to traverse all dataset nodes and find the connected node with the maximum coverage.

Effect of Resolutions. Fig. 21 presents the search time as the θ increases. We can see that the search time of the four algorithms gradually increases, but MSDS always maintains the best search performance. Moreover, the search time of the SG algorithm increases more rapidly than that of the other two algorithms. This is because the number of elements in each spatial set increases as the θ increases and pairwise coverage computation and comparison will take more time.

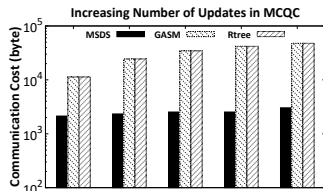


Fig. 24. Communication cost with the increase of updates.

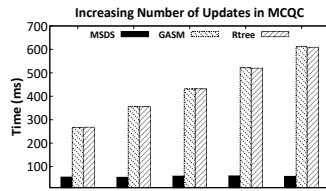


Fig. 25. Transmission time with the increase of updates.

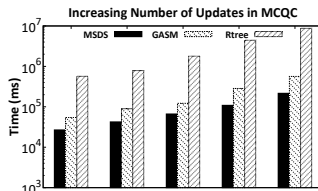


Fig. 26. Search time with the increase of updates.

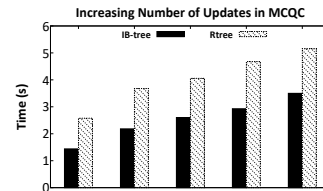


Fig. 27. Index updating time with the increase of updates.

Effect of Number of Queries. Fig. 22 shows the search time as the number of queries increases in MCQC. Similarly to MIQ, we can see that the MSDS still has the best performance and is not affected much. This is consistent with the fact we point out that the dataset graph significantly reduces the MCQC search time.

Effect of Connectivity Thresholds. We increase δ to investigate the search performance of the four algorithms. From Fig. 23, we can see with the increase of δ , the search time of the four algorithms gradually increases, among which MSDS consistently outperforms the other three algorithms. That is because, in MSDS, we construct the dataset graph for the different δ in advance of the search. Thus, when a query request comes in, we only need to search once in IBtree, and then we can find the greedy set based on the dataset graph.

8.4.2 Efficiency of Communication

Similar to the dynamic search in MIQ, we update the dataset in batch and gradually increase the number of updates to compare the communication cost and search time of three algorithms, where MSDS applied the dynamic search strategy, and the other two algorithms use the static search. Here, we do not show the SG results in the subsequent figures. The reason is that the overall search time of SG being far more than the other algorithms when the data set is updated frequently.

Communication Cost and Transmission Time. Figs. 24 and 25 present the communication cost and network transmission time of three algorithms. We can observe that with the increase of updates, the number of bytes transmitted by static search increases linearly compared with dynamic search. The reason is that dynamic search only needs to transmit the query request once and returns a new update result when the query result is updated. In contrast, the static search requires repeated transmission of query requests and query results to the interaction center for aggregation operations. Correspondingly, since the transfer time is proportional to the bytes transferred, the transfer time of dynamic searches is more rapid than that of the other two algorithms.

Search and Index Update Time. Similarly, Fig. 26 shows the search time as the number of updates increases in MCQC. We can observe that MSDS achieves the best search performance compared with the other two algorithms, which indicates that the dynamic search can effectively improve search efficiency. In addition, Fig. 27 shows the index updating time as the number of updates increases. We can see that the updating time of the Rtree is slower than IBtree. This is because Rtree spends part of its time maintaining tree balance in addition to building tree indexes.

9 CONCLUSIONS

This paper mainly studied spatial dataset join and union searches over multiple data sources and defined two novel search paradigms

called MIQ and MCQC. To solve them, we developed a unified MSDS framework. Firstly, we proposed an IBtree index to organize the datasets of each data source efficiently and built a global index for the interaction center to reduce communication costs. Secondly, in the static search, we designed a search algorithm based on IBtree and two heuristic greedy algorithms to accelerate the MIQ and MCQC, respectively. When the datasets are constantly updated, we designed an index dynamic updating strategy and top- k dynamic search methods to maintain up-to-date results. The experimental results showed that our MSDS framework improves search performance and reduces communication costs. An interesting future research direction is to explore the spatial dataset search based on the data pricing to return the optimal dataset combination that satisfies users' requests under a budget.

REFERENCES

- [1] Geoblacklight. <https://geoblacklight.org/>.
- [2] OpenGeoHub. <https://github.com/OpenGeoHub/>.
- [3] Opengeometadata. <https://github.com/OpenGeoMetadata/>.
- [4] M. Adelfio, S. Nutanong, and H. Samet. Similarity search on a large collection of point sets. In *SIGSPATIAL*, pages 132–141, 2011.
- [5] A. Aji, F. Wang, H. Vo, R. Lee, Q. Liu, X. Zhang, and J. H. Saltz. Hadoop-gis: A high performance spatial data warehousing system over mapreduce. *PVLDB*, 6(11):1009–1020, 2013.
- [6] A. Akdogan, U. Demiryurek, F. B. Kashani, and C. Shahabi. Voronoi-based geospatial query processing with mapreduce. In *CloudCom*, pages 9–16, 2010.
- [7] M. E. Ali, S. S. Eusuf, K. Abdullah, F. M. Choudhury, J. S. Culpepper, and T. Sellis. The maximum trajectory coverage query in spatial databases. *PVLDB*, 12(3):197–209, 2018.
- [8] A. Arasu, V. Ganti, and R. Kaushik. Efficient exact set-similarity joins. In *VLDB*, pages 918–929, 2006.
- [9] R. J. Bayardo, Y. Ma, and R. Srikant. Scaling up all pairs similarity search. In *WWW*, pages 131–140, 2007.
- [10] A. Bogatu, A. Fernandes, N. W. Paton, and N. Konstantinou. Dataset discovery in data lakes. In *ICDE*, pages 709–720, 2020.
- [11] P. Bours, S. Ge, and N. Mamoulis. Spatio-textual similarity joins. *PVLDB*, 6(1):1–12, 2012.
- [12] D. Brickley, M. Burgess, and N. F. Noy. Google dataset search: Building a search engine for datasets in an open web ecosystem. In *WWW*, pages 1365–1375, 2019.
- [13] S. Castelo, R. Rampin, A. S. R. Santos, A. Bessa, F. Chirigati, and J. Freire. Auctus: A dataset search engine for data discovery and augmentation. *PVLDB*, 14(12):2791–2794, 2021.
- [14] A. Chapman, E. Simperl, L. Koesten, G. Konstantinidis, L. Ibáñez, E. Kacprzak, and P. Groth. Dataset search: a survey. *VLDBJ*, 29(1):251–272, 2020.
- [15] L. Chen, G. Cong, and X. Cao. An efficient query indexing mechanism for filtering geo-textual data. In *SIGMOD*, pages 749–760, 2013.
- [16] L. Chen, G. Cong, X. Cao, and K. Tan. Temporal spatial-keyword top-k publish/subscribe. In *ICDE*, pages 255–266, 2015.
- [17] R. Cohen and L. Katzir. The generalized maximum coverage problem. *Inf. Process. Lett.*, 108(1):15–22, 2008.

- [18] B. Ding and A. C. König. Fast set intersection in memory. *PVLDB*, 4(4):255–266, 2011.
- [19] M. Dixit, O. Cats, T. Brands, N. van Oort, and S. Hoogendoorn. Perception of overlap in multi-modal urban transit route choice. *Transportmetrica A: Transport Science*, 19(2):2005180, 2023.
- [20] Y. Dong, K. Takeoka, C. Xiao, and M. Oyamada. Efficient joinable table discovery in data lakes: A high-dimensional similarity-based approach. In *ICDE*, pages 456–467, 2021.
- [21] A. Eldawy and M. F. Mokbel. Spatialhadoop: A mapreduce framework for spatial data. In *ICDE*, pages 1352–1363, 2015.
- [22] R. C. Fernandez, Z. Abedjan, F. Koko, and et al. Aurum: A data discovery system. In *ICDE*, pages 1001–1012, 2018.
- [23] I. Gargantini. An effective way to represent quadtrees. *Commun. ACM*, 25(12):905–910, 1982.
- [24] A. Guttman. R-trees: A dynamic index structure for spatial searching. In *SIGMOD*, pages 47–57, 1984.
- [25] D. He, T. Zhou, X. Zhou, and J. Kim. An efficient algorithm for maximum trajectory coverage query with approximation guarantee. *TITS*, 23(12):24031–24043, 2022.
- [26] T. Hervey, S. Lafia, and W. Kuhn. Search facets and ranking in geospatial dataset search. *177:5:1–5:15*, 2021.
- [27] D. S. Hochbaum and A. Pathria. Analysis of the greedy approach in problems of maximum k-coverage. *Naval Research Logistics*, 45(6):615–627, 1998.
- [28] J. Houston, G. Zuidhof, L. Bergamini, and et al. One thousand and one hours: Self-driving motion prediction dataset. In *CoRL*, volume 155, pages 409–418, 2020.
- [29] S. Khuller, A. Moss, and J. Naor. The budgeted maximum coverage problem. *Inf. Process. Lett.*, 70(1):39–45, 1999.
- [30] G. Li, Y. Wang, T. Wang, and J. Feng. Location-aware publish/subscribe. In *SIGKDD*, pages 802–810, 2013.
- [31] D. Mottin, M. Lissandrini, Y. Velegrakis, and T. Palpanas. Exemplar queries: a new way of searching. *VLDBJ*, 25(6):741–765, 2016.
- [32] F. Nargesian, E. Zhu, K. Q. Pu, and R. J. Miller. Table union search on open data. *PVLDB*, 11(7):813–825, 2018.
- [33] P. Ouellette, A. Sciortino, F. Nargesian, B. G. Bashardoost, E. Zhu, K. Q. Pu, and R. J. Miller. RONIN: data lake exploration. *PVLDB*, 14(12):2863–2866, 2021.
- [34] J. Peng, H. Wang, J. Li, and H. Gao. Set-based similarity search for time series. In *SIGMOD*, pages 2039–2052, 2016.
- [35] B. Qiao, B. Hu, J. Zhu, G. Wu, C. G. Giraud-Carrier, and G. Wang. A top-k spatial join querying processing algorithm based on spark. *Inf. Syst.*, 87, 2020.
- [36] E. K. Rezig, A. Bhandari, A. Fariha, B. Price, A. Vanterpool, V. Gadepally, and M. Stonebraker. DICE: data discovery by example. *PVLDB*, 14(12):2819–2822, 2021.
- [37] N. Ta, G. Li, Y. Xie, C. Li, S. Hao, and J. Feng. Signature-based trajectory similarity join. *TKDE*, 29(4):870–883, 2017.
- [38] V. V. Vazirani. *Approximation algorithms*. 2001.
- [39] M. Vlachos, M. Hadjieleftheriou, D. Gunopulos, and E. J. Keogh. Indexing multi-dimensional time-series with support for multiple distance measures. In *SIGKDD*, pages 216–225, 2003.
- [40] K. Wang, J. Han, B. Tu, J. Dai, W. Zhou, and X. Song. Accelerating spatial data processing with mapreduce. In *ICPADS*, pages 229–236, 2010.
- [41] S. Wang, Z. Bao, J. S. Culpepper, T. Sellis, M. Sanderson, and X. Qin. Answering top-k exemplar trajectory queries. In *ICDE*, pages 597–608, 2017.
- [42] S. Wang, Z. Bao, J. S. Culpepper, Z. Xie, Q. Liu, and X. Qin. Torch: A search engine for trajectory data. In *SIGIR*, pages 535–544, 2018.
- [43] S. Wang, Y. Sun, C. Musco, and Z. Bao. Public transport planning: When transit network connectivity meets commuting demand. In *SIGMOD*, pages 1906–1919, 2021.
- [44] X. Wang, Y. Zhang, W. Zhang, X. Lin, and W. Wang. Ap-tree: Efficiently support continuous spatial-keyword queries over stream. In *ICDE*, pages 1107–1118, 2015.
- [45] D. Xie, F. Li, and J. M. Phillips. Distributed trajectory similarity search. *PVLDB*, 10(11):1478–1489, 2017.
- [46] W. Yang, S. Wang, Y. Sun, and Z. Peng. Fast dataset search with earth mover’s distance. *PVLDB*, 15(11):2517–2529, 2022.
- [47] S. You, J. Zhang, and L. Gruenwald. Large-scale spatial join query processing in cloud. In *ICDE*, pages 34–41, 2015.
- [48] H. Yuan and G. Li. Distributed in-memory trajectory similarity search and join on road network. In *ICDE*, pages 1262–1273, 2019.
- [49] E. T. Zacharitou, H. Doraiswamy, A. Ailamaki, C. T. Silva, and J. Freire. Gpu rasterization for real-time spatial aggregation over arbitrary polygons. *PVLDB*, 11(3):352–365, 2017.
- [50] J. Zhang. Multi-source remote sensing data fusion: status and trends. *International Journal of Image and Data Fusion*, 1(1):5–24, 2010.
- [51] J. Zhang, S. You, and L. Gruenwald. Parallel selectivity estimation for optimizing multidimensional spatial join processing on gpus. In *ICDE*, pages 1591–1598, 2017.
- [52] E. Zhu, D. Deng, F. Nargesian, and R. J. Miller. Josie: Overlap set similarity search for finding joinable tables in data lakes. In *SIGMOD*, pages 847–864, 2019.
- [53] M. Zhu, D. Papadias, J. Zhang, and D. L. Lee. Top-k spatial joins. *TKDE*, 17(4):567–579, 2005.



Wenzhe Yang received the BE degree and ME degree in computer science and technology from Jilin University, China in 2017, 2020, respectively. She is currently working toward the Ph.D degree in the computer science and technology, School of Computer Science, Wuhan University, China. Her research interests mainly include spatial database, spatial data sharing, spatial dataset search.



Sheng Wang received the BE degree in information security, ME degree in computer technology from Nanjing University of Aeronautics and Astronautics, China in 2013 and 2016, and Ph.D. from RMIT University in 2019. He is a professor at the School of Computer Science, Wuhan University. His research interests mainly include spatial databases. He has published full research papers on top database and information systems venues as the first author, such as TKDE, SIGMOD, PVLDB, and ICDE.



Yuan Sun is a Lecturer in Business Analytics and Artificial Intelligence at La Trobe University, Australia. He received his BSc in Applied Mathematics from Peking University, China, and his PhD in Computer Science from The University of Melbourne, Australia. His research interest is on artificial intelligence, machine learning, operations research, and evolutionary computation. His research has contributed significantly to the emerging area of leveraging machine learning for combinatorial optimisation.



Zhiyu Chen works as an applied scientist at Amazon. He received his BE degree in computer science from Nanjing University of Aeronautics and Astronautics, China in 2015, and his Ph.D. from Lehigh University in 2022. His research interests include data mining, machine learning, information retrieval and natural language processing. He has published multiple research papers in top conferences such as ICML, SIGIR, WSDM, TheWebConf, EMNLP and ACL.



Zhiyong Peng received the BSc degree from Wuhan University, in 1985, the MEng degree from the Changsha Institute of Technology of China, in 1988, and the PhD degree from the Kyoto University of Japan, in 1995. He is a professor of computer school, the Wuhan University of China. His research interests include complex data management, web data management, and trusted data management.